

1 **T cell Homeostatic Imbalance in Placentae from Women Infected with HIV in the absence of**

2 **Vertical Transmission.**

3

4 Nadia M. Ikumi¹, Komala Pillay^{3,4}, Tamara Tilburgs^{5,6}, Thokozile R. Malaba⁷, Sonwabile Dzanibe¹

5 Elizabeth Ann L Enninga⁸, Rana Chakraborty^{8,9,10}, Mohammed Lamorde¹¹, Landon Myer⁷, Saye

6 Khoo¹², Heather B Jaspan¹ and Clive M. Gray^{1,2,3*}, for the DolPHIN-2 Study Group

7

8 ¹Division of Immunology, Institute of Infectious Disease and Molecular Medicine, University of Cape
9 Town, South Africa.

10 ²Department of Pathology, University of Cape Town, Cape Town, South Africa

11 ³National Health Laboratory Services, Groote Schuur Hospital, Cape Town, South Africa

12 ⁴Division of Anatomical Pathology, Department of Pathology, University of Cape Town, Cape Town,
13 South Africa

14 ⁵Division of Immunobiology, Center for Inflammation and Tolerance, Cincinnati Children's Hospital,
15 Cincinnati OH 45229, USA

16 ⁶Department of Pediatrics, University of Cincinnati College of Medicine, Cincinnati OH 45229, USA

17 ⁷Division of Epidemiology and Biostatistics, School of Public Health and Family Medicine, University
18 of Cape Town, Cape Town, South Africa

19 ⁸Department of Obstetrics and Gynecology, Mayo Clinic, Rochester, MN 55905

20 ⁹Department of Pediatric and Adolescent Medicine, Mayo Clinic College of Medicine and Science,
21 Minnesota, USA

22 ¹⁰Department of Immunology, Mayo Clinic, Rochester, MN 55905

23 ¹¹Infectious Diseases Institute, College of Health Sciences, Makerere University, Kampala, Uganda

24 ¹²Molecular and Clinical Pharmacology, University of Liverpool, Liverpool, UK; Royal Liverpool and
25 Broadgreen University Hospitals NHS Trust, Liverpool, UK

26 **Running title:** Altered T cell immunity during HIV in the placenta

27

28 **Conflict of interest statement**

29 The authors have declared that no conflict of interest exists.

30

31 ***Corresponding Author**

32 Clive M Gray, Division of Immunology, Institute of Infectious Disease and Molecular Medicine,

33 Falmouth Building, Faculty of Health Sciences, University of Cape Town, Anzio Road, Observatory,

34 Cape Town, South Africa, 7925; Tel: +27 21 406 6616; Email: clive.gray@uct.ac.za

35

36 **Word count:** Abstract: 200 words, Lay abstract: 192 words; Main text 3490; 47 references; 5 Figures

37 and 2 Tables; supplementary figures <25MB.

38 **ABSTRACT**

39 **Background:** Implementation of Option B+ antiretroviral therapy (ART) has significantly lowered
40 vertical transmission rates but has also increased numbers of HIV-exposed uninfected children
41 (HEU), who remain vulnerable to morbidities. Here, we investigated whether altered immune status
42 in HEU originates in the placenta.

43 **Methods:** We analyzed T cells from term placentae decidua and villous tissue and paired cord blood
44 from pregnant women living with HIV (PWLWH) who initiated ART late in pregnancy (n=21) with HIV
45 negative controls (n=9).

46 **Results:** Placentae from PWLWH showed inverted CD4:CD8 ratios and higher proportions of tissue
47 resident CD8+ T cells in villous tissue relative to control placentae. CD8+ T cells in the fetal
48 capillaries, which were of fetal origin, positively correlated with maternal plasma viraemia prior to
49 ART initiation, implying that imbalanced T cells persisted throughout pregnancy. Additionally, the
50 expanded memory differentiation of CD8+ T cells was confined to the fetal placental compartment
51 and cord blood, but was not observed in the maternal decidua.

52 **Conclusion:** T cell homeostatic imbalance in the blood circulation of PWLWH is reflected in the
53 placenta. The placenta may be a causal link between HIV-induced maternal immune changes during
54 gestation and altered immunity in newborn infants in the absence of vertical transmission.

55

56 **Keywords:** T cells, placenta, HIV, prolonged exposure, placenta pathology

57

58

59 **Lay Summary**

60 The effective prevention of HIV transmission during pregnancy with the rollout of antiretroviral
61 therapy (ART) has resulted in increased numbers of HIV-exposed uninfected children (HEU). These
62 children are vulnerable to infections and health problems and they have altered cellular immune
63 systems at birth. We investigated whether these immune alterations may originate in the placenta,
64 as this fetal organ maintains life during pregnancy. Do immune alterations in the newborn child
65 originate in the placenta? After collecting placentae at term from pregnant women living with HIV
66 (PWLWH), who started ART in the third trimester ($n=21$) and from HIV negative controls ($n=9$), we
67 isolated T cells from dissected placental tissue and matching cord blood. Placentae from PWLWH
68 showed inverted CD4:CD8 ratios in the placenta and cord blood with higher numbers of CD8+ T cells
69 in the fetal part of the placenta. These CD8+ T cells mirrored events in the blood circulation of the
70 mother and the altered balance of T cell immunity in the PWLWH was reflected in the placenta.
71 Accordingly, the placenta may be a pivotal link between HIV-induced maternal immune changes and
72 altered immunity in newborn infants in the absence of vertical transmission.

73

74 **Background**

75 In adults, HIV causes severe immune dysregulation, characterized by systemic depletion of CD4+ T
76 cells, increased HIV-1 specific CD8+ T cells, inflammation and a progressive failure of the immune
77 system[1–3]. Initiation of ART has been shown to augment HIV-specific CD4+ T cell responses, but
78 normalization of the CD4:CD8 T cell ratio does not occur in a large proportion of HIV positive
79 individuals[4]. In pregnant women living with HIV (PWLWH), pregnancy is not associated with HIV
80 disease progression, although it has been associated with functional impairment of systemic effector
81 T cells and an overall altered response against HIV control[5,6].

82

83 Placentae from PWLWH exhibit increased signs of inflammation and injury affecting maternal
84 vasculature and circulation[7,8]. Although the maternal and fetal circulation within the placenta
85 takes place in distinct compartments, there is evidence that maternal HIV infection impacts the fetal
86 immune system. HIV-unexposed uninfected children (HUU) have an almost completely naïve T cell
87 repertoire, but at birth HIV-exposed uninfected children (HEU) can have increased proportions of
88 differentiated immune cells suggestive of antigen experience *in utero*[9,10]. This scenario raises the
89 question of how HIV exposure *in utero* potentially creates perturbations of immunity in HEU[11,12].

90

91 In healthy human pregnancies, T cells in the placenta have been shown to constitute approximately
92 5-20% of total leukocytes in the decidua and this proportion increases up to over 40% at
93 term[13,14]. CD8+ T cells are the most abundant subset and are important in promoting embryo
94 implantation and providing immune protection against infection[15,16]. CD4+ T cell subsets have a
95 number of key roles including the establishment and maintenance of fetal-maternal (FM)
96 tolerance[17,18]. Fetus-specific CD4+ Tregs have been shown to migrate towards the FM interface
97 where they are enriched to guard against breakdown in FM tolerance[18]. In contrast, the presence
98 of CD8+ T cells in the villous tissue is often associated with villitis of unknown etiology (VUE), an

99 inflammatory state of the placenta characterized by the infiltration of maternal CD8+ T cells and
100 macrophages into the villi[19,20].

101 To test the hypothesis that maternal HIV infection is associated with disruption of T cell homeostasis
102 in the placenta and cord blood from HEU newborns, we examined term placentae from PWLWH
103 from a randomized trial in pregnant mothers initiating dolutegravir versus efavirenz-containing
104 therapy in the third trimester (DolPHIN-2: NCT03249181)[21], as well as pregnant women not living
105 with HIV (PWNLHIV), serving as controls. We show that placentae from PWLWH have inverted
106 CD4:CD8 ratios with higher CD8+ T cells in villous tissue relative to control placentae contributing to
107 T cell homeostatic imbalance in the placenta at birth.

108

109

110

111 **Methods**

112 *Cohort*

113 We included 21 placentae with 9 paired cord blood samples from PWLWH and HEU and 9 placentae
114 from PWNLHIV with 5 cord blood samples from HUU in this study. The PWLWH group was nested in
115 the DolPHIN-2 study and recruited from the Gugulethu Community Health Centre, Cape Town[21].
116 HIV negative controls were enrolled nearby from the Khayelitsha Site B Midwife Obstetric Unit, Cape
117 Town. All placentae were from term deliveries (>37 weeks' gestation).

118

119 *Clinical Data collection*

120 As part of DolPHIN-2, maternal systemic CD4 T cell counts were measured at ART initiation and
121 plasma viral load (VL) copies were measured at screening, enrolment and ART initiation (visit 1), one
122 week after ART initiation (visit 2), four weeks after ART initiation (visit 3), thirty-six weeks' GA (visit
123 4) and approximately ± 14 days after delivery (visit 5). The level of detection was 50 copies per
124 ml[21].

125

126 *Placenta and cord blood processing.*

127 Cells were isolated from each placenta as previously described[22] and illustrated in Figure 1.
128 Placentae were collected in RPMI 1640 supplemented with 10% fetal calf serum (FCS) and
129 penicillin/streptomycin at room temperature and processing was performed within six hours of
130 delivery. Briefly, each placenta was macroscopically inspected and dissected to obtain the decidua
131 parietalis, basalis and villous tissue. The sections were rinsed in phosphate-buffered saline (PBS) to
132 remove maternal blood. Enzymatic lymphocyte isolation was performed using 0.2% Collagenase I
133 and 0.02% DNase I in RPMI 1640 at 37°C for 75 minutes. We then obtained the lymphocyte fraction
134 following Percoll density centrifugation at the 70-45% interface and incubated the cells with violet
135 amine reactive viability dye (VIVID, ThermoFisher) according to manufacturer's instructions. The cells
136 were then fixed using BD FACS™ lysing solution, cryopreserved in 90% FCS - 10% Dimethyl sulfoxide

137 (DMSO) and stored in liquid nitrogen until analysis. Cord blood mononuclear cells were isolated on
138 Ficoll, fixed and cryopreserved in the same fashion as placental lymphocytes.

139

140 *Placenta pathology*

141 Placentae were fixed in 10% buffered formalin prior to histopathology examination at Red Cross
142 Memorial Children's Hospital, Cape Town, South Africa. Specimens were macroscopically examined
143 and samples from the umbilical cord, placental membranes and placental disk were obtained based
144 on the Amsterdam Placental Workshop Group Consensus Statement.[23] Briefly, four blocks were
145 prepared from each placenta; including a roll of the placental membranes, two cross sections of the
146 umbilical cord; and full-thickness sections of the placental parenchyma including one from the cord
147 insertion. Tissue sections were 3-5 μ m thick and were stained with haematoxylin and eosin for
148 routine histological examination. Placentae were examined for features of prolonged meconium
149 exposure, chorioamnionitis with or without a maternal or fetal inflammatory response[24,25],
150 maternal vascular malperfusion (MVM) with decidual vasculopathy, and in the absence of decidual
151 vasculopathy, MVM was indicated by a small placenta for gestational age accompanied by at least
152 two villous changes (villous infarct, retroplacental haematoma, accelerated villous maturation or
153 distal villous hypoplasia). In the case of normal placenta weights for gestational age, at least 3-4
154 villous features were noted to be placed in the category of MVM[26]. Chronic deciduitis was defined
155 as abnormal infiltration of lymphocytes and plasma cells in the decidua[23].

156

157 *Flow cytometry*

158 Placental and cord blood cells were labeled with fluorochrome-conjugated monoclonal antibodies:
159 CD3 (Clone UCHT1), CD4 (Clone SK3), CD8 (Clone SK1), CD45RA (Clone H100), CD28 (Clone CD28.2),
160 CD14 (Clone MHCD1417) and CD45 (Clone MHCD4530). Samples were acquired using an LSR II flow
161 cytometer (BD Biosciences). Total CD4+ and CD8+ T cells were expressed as a proportion of CD3+ T
162 cells gated from the viable CD45+ CD14- cells (Supplementary Figure 1).

163 *Immunohistochemistry*

164 Formalin fixed paraffin embedded (FFPE) placenta tissue blocks were cut into 5 µM sections and
165 stained with CD8 (Clone C8/144B), with tonsillar tissue serving as a control. Briefly, the slides were
166 baked overnight at 56°C and rehydrated in xylene followed by varying concentrations of alcohol and
167 then incubated in 3% hydrogen peroxide. Heat-mediated antigen retrieval was performed using an
168 EDTA buffer (pH9). The slides were then incubated with 1% Bovine Serum Albumin (BSA) and stained
169 with the primary antibody anti-CD8. The images were acquired on Zeiss Axioskop 200 upright
170 Fluorescence microscope with an AxioCam high resolution colour (HRC) camera.

171

172 *Fluorescence in situ hybridization (FISH)*

173 We used five placental samples from male fetuses to identify the origin of the infiltrating
174 lymphocytes by FISH. Briefly, the slides were baked at 90°C for 15 minutes, deparaffinized in xylene,
175 dehydrated in 100% ethanol and then placed in 10mM Citric Acid (pH 6.0). The slides were then
176 dehydrated in varying concentrations of ethanol (70%, 85% and 100%). We then applied a working
177 solution of DXZ1/DYZ3 (Abbott Laboratories, Des Plaines, IL, USA) to the target areas, co-denatured
178 with a ThermoBrite (Abbott Laboratories) and hybridized overnight at 37°C. The slides were then
179 counter stained with 4'-6'-diamidino-2-phenylindole (DAPI) (Vector Laboratories). Tissue samples
180 were scanned and the qualitative result was determined based on observed signal patterns by
181 CytoVision (Leica Biosystems, Germany).

182

183 *Statistics*

184 All flow cytometry data were analyzed using FlowJo version 10 (Treestar). Statistical analyses were
185 performed using Prism version 8 (Graphpad Software, San Diego, CA), STATA version 12.0 (Stata
186 Corporation, College Station, Texas, USA) or R[27]. Immunohistochemistry tissue cell counts for each
187 tissue section were obtained by counting the total number of positive CD8+ T cells on the
188 immunostained slides (40x magnification) using Image J Fiji version 2 (WS Rasband, National

189 Institute of Health, Bethesda, MD). Tests of significance were performed using Mann-Whitney *U* and
190 Kruskal-Wallis tests for intergroup comparisons. The associations between cell proportions and viral
191 load or CD4 T cell counts were assessed using simple linear regression. All bivariate analyses
192 including maternal and infant characteristics, and placental pathology stratified by HIV-exposure or
193 by ART regimen were compared using Chi² or Fisher's exact test and Wilcoxon rank-sum tests.

194

195 *Study approval*

196 The study protocol, informed consent forms and all data collection tools were approved by the
197 University of Cape Town, Faculty of Health Sciences Research Ethics Committee. Written and signed
198 informed consent was obtained from all participants, including collection of placentae prior to study
199 inclusion.

200

201 **Results**

202 *Participant Characteristics.*

203 Maternal and newborn infant characteristics are shown in Table 1. No differences in maternal age
204 were noted between PWNLHIV and PWLWH at enrolment, with the median gestational age (GA)
205 being 30 weeks and 28 weeks between the groups. PWLWH were more likely to be multigravida
206 ($p=0.003$). Median GA at delivery was 40 weeks in PWNLHIV and 39 weeks in the PWLWH ($p=0.03$)
207 and there was a tendency toward lower birthweight in HEU ($p=0.07$). Among the 21 PWLWH, 16
208 (76.2%) were randomised to receive efavirenz (EFV + TDF + 3TC) and 5 (23.8%), dolutegravir (DTG +
209 TDF + 3TC), shown in Supplementary Table 1. Median CD4 count at ART initiation was 358 cells/mm³
210 (IQR 278 – 477), with no difference between ART groups (Supplementary Table 2). The median VL at
211 ART initiation was $4.54 \log_{10}$ RNA copies/ml (IQR 3.85 – 4.80) in the EFK group versus $3.83 \log_{10}$ RNA
212 copies/ml (3.49 – 3.83) in the DTG group, with a combined viraemia of $4.28 \log_{10}$ RNA copies/ml
213 (Supplementary Table 2). Both ART groups were on treatment for a median of 84 days IQR (44 - 105)
214 and women in the DTG arm achieved viral suppression at a faster rate (cut off ≤ 50 copies/ml or 1.69

215 \log_{10} RNA copies/ml) at 4 weeks versus 2 weeks after delivery (Supplementary Table 2 and [21]). For
216 the purposes of this study, we combined the placentae from two ART groups, as there were only 5
217 collected from the DTG arm.

218

219 *Placental weight is altered by HIV.*

220 Table 2 shows placenta characteristics and pathology stratified by HIV status. PWNLHIV had
221 significantly larger placentae (468g, IQR 426 - 533) compared to the PWLWH (394g, IQR 343 - 469;
222 p=0.02), with 38% of placentae in PWLWH being <10th percentile weight-for-gestation compared to
223 0% in PWNLHIV. These differences were also reflected in the fetal-placental (FP) ratios, where all
224 cases with FP ratios > 90th percentile were in the PWLWH cases (p=0.02). Placental histopathology
225 identified 2 cases (9.5%) of chronic deciduitis and 6 cases (28.6%) of MVM, all in the PWLWH. There
226 were no significant differences in the incidence of meconium exposure and chorioamnionitis
227 between PWLWH and PWNLHIV, and there was no evidence of villitis of unknown etiology (VUE) in
228 any of the placentae. There were no significant differences in the placental weight, FP ratio and
229 placental pathology between the two ART groups (Supplementary Table 3).

230

231 *HIV infection during pregnancy alters placental CD4+ and CD8+ T cell proportions.*

232 Figure 2A shows significantly lower proportions of CD4+ T cells in decidua parietalis and basalis, but
233 not in the villous tissue, comparing placentae from PWLWH with PWNLHIV. The proportion of CD8+
234 T cells was significantly increased (Figure 2A) in all three placental compartments resulting in
235 significantly lower CD4:CD8 T cell ratios in the three placental tissues from PWLWH (Figure 2B).
236 Notably, the inverted CD4:CD8 ratio in villous tissue was due to the increased CD8+ T cells in the
237 villous tissue. The inverted CD4:CD8 ratio was partially reflected in cord blood from HEU (Figures
238 2B). No differences were identified in T cell proportions when stratified by the different ART
239 regimens (Supplementary Figure 2).

240

241 Maternal absolute peripheral blood CD4 T cell counts, measured pre-ART at a median of 28 weeks'
242 gestation, positively correlated with the proportion of CD4+ T cells in the decidua and negatively
243 correlated with the proportion of CD8+ T cells in decidua and villous tissue (Figure 2C and D). A
244 similar trend, without significance, was observed in cord blood. Thus, the inverted placental tissue
245 CD4:CD8+ T cell ratios appeared to reflect the maternal peripheral immune status but was mirrored
246 to a lesser extent in the cord blood of HEU. This correlation was temporally dissociated, where
247 correlations were made between blood measured at 28 weeks and placentae measured at 38-40
248 weeks of gestation, suggesting that inverted T cell ratios persisted throughout pregnancy.

249

250 *Maternal viral load prior to ART initiation correlates with placental, but not cord blood, CD4+ and*
251 *CD8+ T cell proportions.*

252 Maternal plasma viraemia dropped precipitously over time from enrolment to delivery (-12 weeks
253 beforehand), where PWLWH receiving DTG decreased at a faster rate (Figure 3A)^[17]. As expected,
254 the enrolment plasma viraemia, ranging from 1.69 - 6.0 log₁₀ RNA copies/ml, significantly inversely
255 correlated with the absolute maternal peripheral blood CD4+ T cell count determined pre-ART, at
256 enrolment (Figure 3B). Interestingly, pre-ART viremia also showed a significant negative correlation
257 with proportions of CD4+ T cells in the decidua parietalis and basalis (Figure 3C) and a positive
258 correlation with CD8+ T cells in the decidua parietalis, basalis and villous tissue at delivery (Figure
259 3D). The association between maternal viral loads over time and the proportions of decidual CD4+
260 and CD8+ T cells were maintained at -8 weeks and -4 weeks before delivery for CD4+ T cells
261 (Supplementary Figure 3) and up to -8 weeks before delivery for CD8+ T cells (Supplementary Figure
262 4). Maternal viremia did not correlate with the proportion of T cells in the cord blood (Figure 3C and
263 3D), suggesting that maternal VL (pre- and post-ART initiation) can influence the homeostatic
264 balance of T cells in the placenta, but not in the “newborn” immune compartment.

265

266

267 *Immunohistochemistry confirms anatomical location and fetal origin of CD8+ T cells in villous tissue.*
268 Analysis of placental villi from 13 PWLWH and 3 PWNLHIV controls showed the presence of CD8+
269 cells in the fetal capillaries (Figure 4A). The numbers of CD8+ T cells positively correlated with pre-
270 ART maternal viremia (Figure 4B), confirming the flow cytometric analysis (Figures 2A, 3D). Using
271 FISH to detect X and Y chromosomes in cells located within the villi from 5 placentae with male
272 births, we confirmed the presence of male (fetal) cells in fetal capillaries (Figure 4C). Thus the
273 immunohistochemistry analysis confirms the anatomical location and fetal origin of the increased
274 proportions of CD8+ T cells in villous tissue. The fetal (male) origin of the CD8+ T cells in placental
275 villi is consistent with the absence of VUE, a lesion that is characterized by maternal immune
276 infiltrates[20,28].

277

278 *HIV exposure increases differentiation of CD8+ T cells in placental villi and fetal cord blood, but not in*
279 *the maternal placental compartments.*

280 CD45RA and CD28 was used to identify the proportions of naïve (CD45RA+CD28+), early
281 differentiated (ED, CD45RA-CD28+), late differentiated (LD, CD45RA-CD28-) and terminally
282 differentiated (TD, CD45RA+CD28-) memory CD4+ and CD8+ T cells from villous tissue and matching
283 cord blood (Figure 5A). We observed significantly lower proportions of naïve CD8+ T cells and
284 significantly higher proportions of LD CD8+ T cells in villous tissue and cord blood of HEU compared
285 to HUU (Figure 5B). The CD4+ T cells in the villous tissue were predominantly of a naïve and ED
286 phenotype while the cord blood cells were predominantly naïve. There were no significant
287 differences in CD4+ T cell differentiation state based on HIV-exposure (Supplementary Figure 5). In
288 addition, no significant differences in the stage of CD4+ and CD8+ T cell differentiation in decidua
289 parietalis and decidua basalis was observed between the HIV groups (Supplementary Figure 6). Thus,
290 the increased differentiation state of CD8+ T cells is confined to the fetal placental and fetal cord
291 blood compartments and not observed in the maternal placental compartments. Interestingly, there

292 was no correlation between maternal pre-ART VL and memory stage of CD8+ T cells in placental
293 villous tissue and cord blood (data not shown).

294

295 **Discussion**

296 We present data from a unique cohort of PWLWH who initiated ART late in pregnancy and show that
297 maternal HIV infection has a clear impact on T cell subsets in the decidua, villous tissue and cord
298 blood. As the decidua and decidual immune cells are of maternal origin, it may not be surprising to
299 find such a footprint[29]. Maternal HIV infection likely affects and kills maternal decidual CD4+ T
300 cells and fewer peripheral blood T cells may traffic to decidual tissue; chemokine gradients have
301 been shown to play a key role in the trafficking of maternal T cells into the decidua during
302 pregnancy[30]. We show that in contrast to the decidua, the inverted CD4:CD8 ratio in the fetal
303 villous tissue was largely due to an increased proportion of CD8+ T cells and not, as observed in the
304 other tissues, due to a decrease in CD4+ T cells. These CD8+ T cells were of an early-late
305 differentiated phenotype, suggestive of previous antigen experience[31,32].

306

307 The human placenta has two circulatory compartments: the utero-placental unit for the trafficking
308 of maternal blood and the feto-placental unit for the fetal blood circulation[33,34]. Approximately
309 40% of the total fetal-placental blood volume exists as a reservoir in the placenta[34]. The cells we
310 characterised in the villous tissue and cord blood are from the feto-placental unit and these villous
311 tissue resident cells are likely predominantly from the placental reservoir. A key question is whether
312 the increased CD8+ T cell differentiation in placental villi and cord blood is due to direct exposure to
313 HIV antigens, presence of other pathogens in placental or fetal compartments (e.g. CMV) or
314 increased levels of other non-infectious inflammatory cues in placentae of PWLWH. There is
315 evidence that despite separation of fetal and maternal circulations, viral particles, structural and
316 core HIV proteins have been shown to cross the placental barrier in the absence of fetal infection
317 leading to altered immune profiles in HEU infants[35,36]. A number of studies have also described
318 HIV-specific T cell responses in HEU infants, postulated to have been primed by exposure to HIV
319 antigens *in utero*[11,37,38]. The magnitude of these responses is greatest soon after birth but are
320 not detected in older HEU children, suggesting that in the absence of continuous exposure these

321 responses wane[10,38]. The lower proportion of naïve cells and increased memory T cells reflected
322 in villous tissue and cord blood mirror previous studies; HEU infants have been shown to have
323 reduced CD4+ T cell numbers and increased CD8+ T cells compared to HUU infants at birth[39,40].
324 HEU infants have also been shown to have lower naïve cells thought to be due to thymic involution
325 and frequent stimulation and expansion of the antigen-specific T cells in an effort to regenerate the
326 T cell pool[41–43]. Whether the same findings would be recapitulated in PWLHIV with
327 preconception suppressed viral loads is unknown.

328

329 Interestingly the elevated proportions of CD8+ T cells found embedded in the placental villous tissue
330 from PWLHIV were shown to be sequestered within the fetal capillaries. Furthermore, these CD8+ T
331 cells within villous tissue were proportional to maternal viremia. The absence of overt VUE
332 corroborates the finding that expanded CD8+ T cell fractions are of fetal and not maternal origin.
333 Previous studies have suggested that the presence of T cells in the villi during normal pregnancy
334 reflect VUE[20]. However, there is emerging evidence, using IHC staining of villi sections from early
335 elective termination placentae, of the presence of CD45+ $\alpha\beta$ T cells, although these cells were
336 undetectable at term[44]. In a separate study, using single cell transcriptomic analysis in placentae
337 from women with or without preterm labour, where there were no reported maternal infections,
338 and villous tissue was shown to contain a mixture of fetal and maternal immune cells[45]. We
339 cannot discount the possibility that there was also a mix of maternal and fetal CD8+ T cells in
340 placental villi in our study.

341

342 Of particular note, women were ART naïve during the first and second trimester and it is likely that
343 prolonged HIV exposure may have contributed to altered placental development and the
344 significantly lower placental weight observed. Interestingly, all cases of maternal vascular
345 malperfusion (MVM) were reported in placentae from HIV-infected women and possibly reflects
346 placental injury affecting maternal vasculature and perfusion and increasing the risk of an adverse

347 birth outcome[26]. We have previously reported on MVM in placentae from PLWHIV on long-term
348 ART, an incidence of about 27% overall, similar to Kalk *et al.* [7,46]. It is likely that HIV and/or ART
349 exposure alters factors involved in vascular development, resulting in placental insufficiency and
350 increased risk of adverse birth outcomes[47].

351

352 In conclusion, we provide evidence that *in utero* exposure to HIV results in an altered immune
353 footprint in both the utero-placental and feto-placental compartments. Despite the initiation of ART
354 in the third trimester, resulting in either full or partial maternal viral suppression by the time of
355 delivery, there was a significant imbalance in term placental T cell homeostasis and to a lesser
356 degree in the cord blood. Our data suggests that the placenta may be a causal link between
357 maternal and neonatal T cell perturbations previously observed in HEU newborns.

358

359 **Author contributions**

360 NMI, ML, SK, LM, HBJ, CMG: Conceptualization and design of the study

361 NMI, TT: Panel design, sample preparation and development of methods

362 KP: Histopathology scoring and interpretation

363 NMI, TRM and SD: Statistical analysis

364 NMI, TT, KP, TM, LM, EAE, RC, HBJ, CMG: Writing the manuscript

365

366 **Funding**

367 This research was supported by a Fellowship to NMI from the AXA Research Fund, Paris. The content

368 is solely the responsibility of the authors and does not necessarily represent the official views of

369 those of the AXA Research Fund. The research is part of the DOLPHIN-2 clinical trial sponsored by

370 UNITAID (ClinicalTrials.gov NCT03249181).

371

372 **Acknowledgments**

373 We wish to thank all the study participants in this study; all the members of the DOLPHIN-2 clinical

374 trial and INFANT placenta study. We also wish to thank Nonzwakazi Bangani, Goitseone Thamae,

375 Michelle Barboure, Berenice Alinde and Lizette Fick for their expert assistance in sample processing

376 and Dr Amsha Ramburan for capturing the FISH images.

377

378

379

380 **Figure Legends**

381 **Figure 1: Lymphocyte isolation from the human placenta**

382 Stepwise isolation of lymphocytes from the human placenta decidua parietalis (DP), decidua basalis (DB) and
383 villous tissue (VT): (1) dissection of the whole placenta; (2) multiple rounds of maternal blood rinsing to avoid
384 contamination followed by enzymatic digestion of each dissected tissue; (3) lymphocyte separation obtained
385 by Percoll density centrifugation; (4) cryopreservation of fixed cells and immunophenotyping using flow
386 cytometry.

387

388 **Figure 2: Proportions of T cells in the placenta and cord blood**

389 **(A)** Box plots (showing medians and interquartile ranges) of CD3+CD4+CD8- T cells and CD3+CD4-CD8+ T cell
390 proportions isolated from the decidua parietalis, decidua basalis, villous tissue and cord blood from Pregnant
391 Women not living with HIV (PWNLHIV) and Pregnant Women living with HIV (PWLWH) and HIV unexposed
392 uninfected (HUU) and HIV exposed uninfected (HEU) cord bloods. **(B)** Box plots (showing medians and
393 interquartile ranges) of CD4:CD8 T cell ratios in the decidua parietalis, decidua basalis, villous tissue and cord
394 blood from Pregnant Women not living with HIV (PWNLHIV) and Pregnant Women living with HIV (PWLWH)
395 and HIV unexposed and uninfected (HUU) and HIV exposed uninfected (HEU) cord bloods. Tests of significance
396 were performed using the Mann-Whitney *U* test. **(C)** Correlation plots between the absolute maternal CD4
397 count at 28 weeks' gestation prior to ART initiation and the proportion of CD4+ T cells isolated from the
398 decidua parietalis, basalis, villous tissue and cord blood. Statistical analysis was performed using the Spearman
399 rank test and the grey shaded areas represent the 95% confidence intervals. **(D)** Correlation plots between the
400 absolute maternal CD4 count at 28 weeks' gestation prior to ART initiation and the proportion of CD8+ T cells
401 isolated from the decidua parietalis, basalis, villous tissue and cord blood. Statistical analysis was performed
402 using the Spearman rank test and the grey shaded areas represent the 95% confidence intervals.

403

404 **Figure 3: Proportions of CD4+ and CD8+ T cells in the placenta and maternal viral load**

405 **(A)** Line plot depicting participant viral load trajectories over time at enrolment and ART initiation (VLV1, 12
406 weeks before delivery), one week after ART initiation (VLV2, 8 weeks before delivery), four weeks after ART
407 initiation (VLV3, 4 weeks before delivery), thirty-six weeks' GA (VLV4, 2 weeks before delivery) and +/- 14 days
408 after delivery (VLV5, +/- 2 weeks after delivery). The women were randomised to receive efavirenz (EFV + TDF

409 + 3TC) (denoted in black) and dolutegravir (DTG + TDF + 3TC) (denoted in blue). **(B)** Correlation plot between
410 maternal systemic absolute CD4 counts at enrolment prior to ART initiation with maternal viral load at
411 enrolment and ART initiation (28 weeks GA). Statistical analysis was performed using the Spearman rank test
412 and the grey shaded area represents the 95% confidence intervals. **(C)** Correlation plots between CD4+ T cell
413 proportions in the placenta and maternal viral load at enrolment and ART initiation (28 weeks GA) in the
414 decidua parietalis, basalis, villous tissue and cord blood. Statistical analysis was performed using the Spearman
415 rank test and the grey shaded area represents the 95% confidence intervals. **(D)** Correlation plots between
416 CD8+ T cell proportions in the placenta and maternal viral load at enrolment and ART initiation (28 weeks GA)
417 in the decidua parietalis, basalis, villous tissue and cord blood. Statistical analysis was performed using the
418 Spearman rank test and the grey shaded area represents the 95% confidence intervals.
419

420 **Figure 4: Anatomical location of CD8+ T cells in the villous tissue**

421 **(A)** Representative immunohistochemical stained images of CD8+ T cells in villous tissue sections denoted in
422 brown dots and black arrows in the villi of placentae from HIV-infected and –uninfected mothers (40x
423 magnification). **(B)** Correlation plot between the density of tissue-bound CD8+ T cells in the villi and maternal
424 viral load at ART initiation (pre-ART). Statistical analysis was performed using the Spearman rank test and the
425 black curved lines represent the 95% confidence intervals. **(C)** Representative Fluorescence in situ
426 Hybridization (FISH) images of lymphocytes (white arrows) in the villous tissue from placentas from male
427 infants. The X chromosome is denoted in green and Y chromosome denoted in red (digitally scanned slides).
428

429 **Figure 5: Memory phenotype of CD4 and CD8 T cells in the Villous Tissue**

430 **(A)** Representative flow cytometry contour plots of Naïve, Early differentiated (ED), Late differentiated (LD)
431 and Terminally differentiated (TD) CD4+ T cells and CD8+ T cells in the villous tissue (VT; upper panel) of
432 placentae from PWNLHIV and PWLWH and cord blood from HIV unexposed and uninfected (HUU) and HIV
433 exposed uninfected (HEU). **(B)** Box plots (showing medians and interquartile ranges) of CD8+ Naïve, Early
434 differentiated (ED), Late differentiated (LD) and Terminally differentiated (TD) T cells in the villous tissue and
435 cord blood from HIV unexposed and uninfected (HUU) and HIV exposed uninfected (HEU). Tests of significance
436 were performed using the Mann-Whitney *U* test.
437

438

439 **Supplementary Figures**

440 **Supplementary Figure 1: Gating strategy to delineate CD3+ T cells**

441 Representative flow cytometry dot plots depicting the gating strategy to delineate CD4+ and CD8+ T cells
442 gated from a live CD45+ CD14- CD3+ population in the placenta.

443

444 **Supplementary Figure 2: Proportions of CD3+ T cells in the placenta and cord blood by ART group**

445 Box plots (showing medians and interquartile ranges) of (A) CD4+ and (B) CD8+ T cells in the decidua parietalis
446 (DPar), decidua basalis (DBas), villous tissue (VTiss) and cord blood (Cblood) from HIV-uninfected (MHIV neg)
447 and infected mothers on efavirenz (EFV) or dolutegravir (DTG) and HIV unexposed and uninfected (HUU) and
448 HIV exposed uninfected (HEU) cord bloods. Tests of significance were performed using the Kruskal-Wallis test.

449

450 **Supplementary Figure 3: Proportions of CD4+ T cells in the placenta, cord blood and maternal viral load**

451 Correlation plots between CD4+ T cell proportions in the placenta and cord blood and maternal viral load one
452 week after ART initiation (visit 2, 8 weeks before delivery), four weeks after ART initiation (visit 3, 4 weeks
453 before delivery) and thirty-six weeks' GA (visit 4, 2 weeks before delivery) in the decidua parietalis, basalis,
454 villous tissue and cord blood. Statistical analysis was performed using the Spearman rank test and the grey
455 shaded area represents the 95% confidence intervals.

456

457 **Supplementary Figure 4: Proportions of CD8+ T cells in the placenta, cord blood and maternal viral load**

458 Correlation plots between CD8+ T cell proportions in the placenta and cord blood and maternal viral load one
459 week after ART initiation (visit 2, 8 weeks before delivery), four weeks after ART initiation (visit 3, 4 weeks
460 before delivery) and thirty-six weeks' GA (visit 4, 2 weeks before delivery) in the decidua parietalis, basalis,
461 villous tissue and cord blood. Statistical analysis was performed using the Spearman rank test and the grey
462 shaded area represents the 95% confidence intervals.

463

464 **Supplementary Figure 5: Memory differentiation of CD4+ T cells in the villous tissue and cord blood**

465 Box plots (showing medians and interquartile ranges) of CD4+ Naïve, Early differentiated (ED), Late
466 differentiated (LD) and Terminally differentiated (TD) T cells in the villous tissue (VT; upper panel) and cord

467 blood (CB; lower panel) from HIV-uninfected (MHIV neg) and infected mothers (MHIV pos) and HIV unexposed
468 and uninfected (HUU) and HIV exposed uninfected (HEU) cord bloods. Tests of significance were performed
469 using the Mann-Whitney *U* test.

470

471 **Supplementary Figure 6: Memory differentiation of CD4 and CD8 T cells in the decidua parietalis and**
472 **decidua basalis**

473 Representative flow cytometry contour plots of Naïve, Early differentiated (ED), Late differentiated (LD) and
474 Terminally differentiated (TD) CD4+ T cells (upper panel) and CD8+ T cells (lower panel) in the decidua
475 parietalis and basalis.

476

477 **Supplementary Figure 7: Memory phenotype of CD4 T cells in the Villous Tissue**

478 Box plots (showing medians and interquartile ranges) of CD4+ and CD8+ Naïve, Early differentiated (ED), Late
479 differentiated (LD) and Terminally differentiated (TD) T cells in the decidua parietalis and basalis from HIV-
480 uninfected (MHIV neg) and infected mothers (MHIV pos). Tests of significance were performed using the
481 Mann-Whitney *U* test.

482

483 **References**

- 484 1. Okoye AA, Picker LJ. CD4 + T-cell depletion in HIV infection: mechanisms of immunological
485 failure. *Immunol Rev* [Internet]. 2013 Jul;254(1):54–64. Available from:
486 <http://doi.wiley.com/10.1111/imr.12066>
- 487 2. Demers KR, Makedonas G, Buggert M, et al. Temporal Dynamics of CD8+ T Cell Effector
488 Responses during Primary HIV Infection. Douek DC, editor. *PLOS Pathog* [Internet]. 2016 Aug
489 3;12(8):e1005805. Available from: <http://dx.plos.org/10.1371/journal.ppat.1005805>
- 490 3. Hileman CO, Funderburg NT. Inflammation, Immune Activation, and Antiretroviral Therapy in
491 HIV. *Curr HIV/AIDS Rep* [Internet]. 2017;14(3):93–100. Available from:
492 <http://www.ncbi.nlm.nih.gov/pubmed/28434169>
- 493 4. Okhai H, Vivancos-Gallego MJ, Hill T, Sabin CA. CD4+:CD8+ T Cell Ratio Normalization and the
494 Development of AIDS Events in People with HIV Starting Antiretroviral Therapy. *AIDS Res*
495 *Hum Retroviruses* [Internet]. 2020 Oct 1;36(10):808–16. Available from:
496 <https://www.liebertpub.com/doi/10.1089/aid.2020.0106>
- 497 5. Cocker ATH, Shah NM, Raj I, et al. Pregnancy Gestation Impacts on HIV-1-Specific Granzyme B
498 Response and Central Memory CD4 T Cells. *Front Immunol* [Internet]. 2020 Feb 11;11.
499 Available from: <https://www.frontiersin.org/article/10.3389/fimmu.2020.00153/full>
- 500 6. Heffron R, Donnell D, Kiarie J, et al. A Prospective Study of the Effect of Pregnancy on CD4
501 Counts and Plasma HIV-1 RNA Concentrations of Antiretroviral-Naive HIV-1–Infected Women.
502 *J AIDS J Acquir Immune Defic Syndr* [Internet]. 2014 Feb;65(2):231–6. Available from:
503 <http://journals.lww.com/00126334-201402010-00016>
- 504 7. Kalk E, Schubert P, Bettinger JA, et al. Placental pathology in HIV infection at term: a
505 comparison with HIV-uninfected women. *Trop Med Int Health* [Internet]. 2017;22(5):604–13.
506 Available from: <http://www.ncbi.nlm.nih.gov/pubmed/28214384>
- 507 8. Mwanyumba F, Gaillard P, Inion I, et al. Placental Inflammation and Perinatal Transmission of
508 HIV-1. *J AIDS J Acquir Immune Defic Syndr* [Internet]. 2002 Mar;29(3):262–9. Available from:

- 509 <http://journals.lww.com/00126334-200203010-00006>
- 510 9. Ono E, Santos AMN dos, Succi RC de M, et al. Imbalance of naive and memory T lymphocytes
511 with sustained high cellular activation during the first year of life from uninfected children
512 born to HIV-1-infected mothers on HAART. *Brazilian J Med Biol Res [Internet]*. 2008
513 Aug;41(8):700–8. Available from:
514 http://www.scielo.br/scielo.php?script=sci_arttext&pid=S0100-879X2008000800011&lng=en&tlang=en
- 516 10. Clerici M, Saresella M, Colombo F, et al. T-lymphocyte maturation abnormalities in uninfected
517 newborns and children with vertical exposure to HIV. *Blood [Internet]*. 2000 Dec
518 1;96(12):3866–71. Available from: <http://www.ncbi.nlm.nih.gov/pubmed/11090071>
- 519 11. Afran L, Garcia Knight M, Nduati E, Urban BC, Heyderman RS, Rowland-Jones SL. HIV-exposed
520 uninfected children: a growing population with a vulnerable immune system? *Clin Exp
521 Immunol [Internet]*. 2014 Apr;176(1):11–22. Available from:
522 <http://www.ncbi.nlm.nih.gov/pubmed/24325737>
- 523 12. Slogrove AL, Powis KM, Johnson LF, Stover J, Mahy M. Estimates of the global population of
524 children who are HIV-exposed and uninfected, 2000–18: a modelling study. *Lancet Glob Heal
525 [Internet]*. 2020 Jan;8(1):e67–75. Available from:
526 <https://linkinghub.elsevier.com/retrieve/pii/S2214109X19304486>
- 527 13. Williams PJ, Searle RF, Robson SC, Innes BA, Bulmer JN. Decidual leucocyte populations in
528 early to late gestation normal human pregnancy. *J Reprod Immunol [Internet]*. 2009
529 Oct;82(1):24–31. Available from:
530 <https://linkinghub.elsevier.com/retrieve/pii/S0165037809004100>
- 531 14. Nancy P, Erlebacher A. T cell behavior at the maternal-fetal interface. *Int J Dev Biol [Internet]*.
532 2014;58(2–4):189–98. Available from: <http://www.ncbi.nlm.nih.gov/pubmed/25023685>
- 533 15. Tilburgs T, Schonkeren D, Eikmans M, et al. Human Decidual Tissue Contains Differentiated
534 CD8 + Effector-Memory T Cells with Unique Properties. *J Immunol [Internet]*. 2010 Oct

- 535 1;185(7):4470–7. Available from:
536 <http://www.jimmunol.org/lookup/doi/10.4049/jimmunol.0903597>
- 537 16. Tilburgs T, Strominger JL. CD8+ effector T cells at the fetal-maternal interface, balancing fetal
538 tolerance and antiviral immunity. *Am J Reprod Immunol [Internet]*. 2013 Apr;69(4):395–407.
539 Available from: <http://www.ncbi.nlm.nih.gov/pubmed/23432707>
- 540 17. Mjösberg J, Berg G, Jenmalm MC, Ernerudh J. FOXP3+ regulatory T cells and T helper 1, T
541 helper 2, and T helper 17 cells in human early pregnancy decidua. *Biol Reprod [Internet]*.
542 2010 Apr;82(4):698–705. Available from: <http://www.ncbi.nlm.nih.gov/pubmed/20018909>
- 543 18. Tilburgs T, Roelen DL, van der Mast BJ, et al. Evidence for a selective migration of fetus-
544 specific CD4+CD25bright regulatory T cells from the peripheral blood to the decidua in
545 human pregnancy. *J Immunol [Internet]*. 2008 Apr 15;180(8):5737–45. Available from:
546 <http://www.ncbi.nlm.nih.gov/pubmed/18390759>
- 547 19. Redline RW. Villitis of unknown etiology: noninfectious chronic villitis in the placenta. *Hum
548 Pathol [Internet]*. 2007 Oct;38(10):1439–46. Available from:
549 <http://www.ncbi.nlm.nih.gov/pubmed/17889674>
- 550 20. Tamblyn JA, Lissauer DM, Powell R, Cox P, Kilby MD. The immunological basis of villitis of
551 unknown etiology – Review. *Placenta [Internet]*. 2013 Oct;34(10):846–55. Available from:
552 <https://linkinghub.elsevier.com/retrieve/pii/S0143400413005894>
- 553 21. Kintu K, Malaba TR, Nakibuka J, et al. Dolutegravir versus efavirenz in women starting HIV
554 therapy in late pregnancy (DOLPHIN-2): an open-label, randomised controlled trial. *Lancet HIV
555 [Internet]*. 2020 May;7(5):e332–9. Available from:
556 <https://linkinghub.elsevier.com/retrieve/pii/S2352301820300503>
- 557 22. Tilburgs T, Crespo AC, van der Zwan A, et al. Human HLA-G+ extravillous trophoblasts:
558 Immune-activating cells that interact with decidual leukocytes. *Proc Natl Acad Sci [Internet]*.
559 2015 Jun 9;112(23):7219–24. Available from:
560 <http://www.pnas.org/lookup/doi/10.1073/pnas.1507977112>

- 561 23. Khong TY, Mooney EE, Ariel I, et al. Sampling and Definitions of Placental Lesions: Amsterdam
562 Placental Workshop Group Consensus Statement. Arch Pathol Lab Med [Internet]. 2016
563 Jul;140(7):698–713. Available from:
564 <http://www.archivesofpathology.org/doi/10.5858/arpa.2015-0225-CC>
- 565 24. Kallapur S, Presicce P, Rueda C, Jobe A, Chouquet C. Fetal Immune Response to
566 Chorioamnionitis. Semin Reprod Med [Internet]. 2014 Jan 3;32(01):056–67. Available from:
567 <http://www.thieme-connect.de/DOI/DOI?10.1055/s-0033-1361823>
- 568 25. Kim CJ, Romero R, Chaemsathong P, Chaiyavit N, Yoon BH, Kim YM. Acute chorioamnionitis
569 and funisitis: definition, pathologic features, and clinical significance. Am J Obstet Gynecol
570 [Internet]. 2015 Oct;213(4):S29–52. Available from:
571 <https://linkinghub.elsevier.com/retrieve/pii/S0002937815009102>
- 572 26. Ernst LM. Maternal vascular malperfusion of the placental bed. APMIS [Internet]. 2018
573 Jul;126(7):551–60. Available from: <http://doi.wiley.com/10.1111/apm.12833>
- 574 27. R Core Team. R: A language and environment for statistical computing [Internet]. Vienna,
575 Austria: R Foundation for Statistical Computing; 2020. Available from: <https://www.r-project.org/>
- 576 28. Enninga EAL, Raber P, Quinton RA, et al. Maternal T Cells in the Human Placental Villi Support
577 an Allograft Response during Noninfectious Villitis. J Immunol [Internet]. 2020 Jun
578 1;204(11):2931–9. Available from:
579 <http://www.jimmunol.org/lookup/doi/10.4049/jimmunol.1901297>
- 580 29. Ander SE, Diamond MS, Coyne CB. Immune responses at the maternal-fetal interface. Sci
581 Immunol [Internet]. 2019 Jan 11;4(31):eaat6114. Available from:
582 <http://immunology.science.org/lookup/doi/10.1126/sciimmunol.aat6114>
- 583 30. Huang Y, Zhu X-Y, Du M-R, Li D-J. Human trophoblasts recruited T lymphocytes and
584 monocytes into decidua by secretion of chemokine CXCL16 and interaction with CXCR6 in the
585 first-trimester pregnancy. J Immunol [Internet]. 2008 Feb 15;180(4):2367–75. Available from:
586 <http://www.jimmunol.org/lookup/doi/10.4049/jimmunol.1201114>

- 587 <http://www.ncbi.nlm.nih.gov/pubmed/18250446>
- 588 31. Tilburgs T, Strominger JL. CD8+ Effector T Cells at the Fetal-Maternal Interface, Balancing
589 Fetal Tolerance and Antiviral Immunity. *Am J Reprod Immunol* [Internet]. 2013
590 Apr;69(4):395–407. Available from: <http://doi.wiley.com/10.1111/aji.12094>
- 591 32. White JT, Cross EW, Kedl RM. Antigen-inexperienced memory CD8+ T cells: where they come
592 from and why we need them. *Nat Rev Immunol* [Internet]. 2017 Jun;17(6):391–400. Available
593 from: <http://www.ncbi.nlm.nih.gov/pubmed/28480897>
- 594 33. Dawe GS, Tan XW, Xiao Z-C. Cell migration from baby to mother. *Cell Adh Migr* [Internet].
595 2007;1(1):19–27. Available from: <http://www.ncbi.nlm.nih.gov/pubmed/19262088>
- 596 34. Acharya G, Sonesson S-E, Flo K, Räsänen J, Odibo A. Hemodynamic aspects of normal human
597 feto-placental (umbilical) circulation. *Acta Obstet Gynecol Scand* [Internet]. 2016
598 Jun;95(6):672–82. Available from: <http://doi.wiley.com/10.1111/aogs.12919>
- 599 35. Nielsen SD, Jeppesen DL, Kolte L, et al. Impaired progenitor cell function in HIV-negative
600 infants of HIV-positive mothers results in decreased thymic output and low CD4 counts.
601 *Blood* [Internet]. 2001 Jul 15;98(2):398–404. Available from:
602 <http://www.ncbi.nlm.nih.gov/pubmed/11435309>
- 603 36. Evans C, Jones CE, Prendergast AJ. HIV-exposed, uninfected infants: new global challenges in
604 the era of paediatric HIV elimination. *Lancet Infect Dis* [Internet]. 2016 Jun;16(6):e92–107.
605 Available from: <https://linkinghub.elsevier.com/retrieve/pii/S1473309916000554>
- 606 37. Kuhn L, Coutsoudis A, Moodley D, et al. T-helper cell responses to HIV envelope peptides in
607 cord blood: protection against intrapartum and breast-feeding transmission. *AIDS* [Internet].
608 2001 Jan 5;15(1):1–9. Available from: <http://www.ncbi.nlm.nih.gov/pubmed/11192849>
- 609 38. Holditch SJ, Eriksson EM, Tarosso LF, et al. Decay kinetics of HIV-1 specific T cell responses in
610 vertically HIV-1 exposed seronegative infants. *Front Immunol* [Internet]. 2011;2:94. Available
611 from: <http://www.ncbi.nlm.nih.gov/pubmed/22566883>
- 612 39. Huo Y, Patel K, Scott GB, et al. Lymphocyte subsets in HIV-exposed uninfected infants and

- 613 HIV-unexposed uninfected infants. *J Allergy Clin Immunol* [Internet]. 2017 Aug;140(2):605-
614 608.e3. Available from: <https://linkinghub.elsevier.com/retrieve/pii/S009167491730338X>
- 615 40. Borges-Almeida E, Milanez HM, Vilela MMS, et al. The impact of maternal HIV infection on
616 cord blood lymphocyte subsets and cytokine profile in exposed non-infected newborns. *BMC*
617 *Infect Dis* [Internet]. 2011 Dec 3;11(1):38. Available from:
618 <http://bmccinfectdis.biomedcentral.com/articles/10.1186/1471-2334-11-38>
- 619 41. Mansoor N, Abel B, Scriba TJ, et al. Significantly skewed memory CD8+ T cell subsets in HIV-1
620 infected infants during the first year of life. *Clin Immunol* [Internet]. 2009 Mar;130(3):280-9.
621 Available from: <http://www.ncbi.nlm.nih.gov/pubmed/18996749>
- 622 42. Akbar AN, Fletcher JM. Memory T cell homeostasis and senescence during aging. *Curr Opin*
623 *Immunol* [Internet]. 2005 Oct;17(5):480-5. Available from:
624 <http://www.ncbi.nlm.nih.gov/pubmed/16098721>
- 625 43. Linton PJ, Dorshkind K. Age-related changes in lymphocyte development and function. *Nat*
626 *Immunol* [Internet]. 2004 Feb 28;5(2):133-9. Available from:
627 <http://www.nature.com/articles/ni1033>
- 628 44. Bonney EA, Pudney J, Anderson DJ, Hill JA. Gamma-Delta T Cells in Midgestation Human
629 Placental Villi. *Gynecol Obstet Invest* [Internet]. 2000;50(3):153-7. Available from:
630 <https://www.karger.com/Article/FullText/10315>
- 631 45. Pique-Regi R, Romero R, Tarca AL, et al. Single cell transcriptional signatures of the human
632 placenta in term and preterm parturition. *Elife* [Internet]. 2019 Dec 12;8. Available from:
633 <https://elifesciences.org/articles/52004>
- 634 46. Ikumi NM, Malaba TR, Komala P, et al. Associating antiretroviral therapy initiated before or
635 during pregnancy with placenta pathology in HIV infected women. *medRxiv*. 2020;
- 636 47. Weckman AM, Ngai M, Wright J, McDonald CR, Kain KC. The Impact of Infection in Pregnancy
637 on Placental Vascular Development and Adverse Birth Outcomes. *Front Microbiol* [Internet].
638 2019 Aug 22;10. Available from:

639 <https://www.frontiersin.org/article/10.3389/fmicb.2019.01924/full>

640

641 **Table 1: Maternal and infant characteristics**

	PWNLHIV N=9	PWLWH N=21	P-Value
Age, years			1.0
≤24	1 (11.1)	2 (9.5)	
25-29	5 (55.6)	11 (52.4)	
≥30	3 (33.3)	8 (38.1)	
Median (IQR)	29 (25 - 31)	29 (26 - 30)	
Median gestation at enrolment	30 (26 - 32)	28 (28 - 31)	0.6
Gravidity			0.003
1	5 (55.6)	1 (4.8)	
2	3 (33.3)	7 (33.3)	
≥3	1 (11.1)	13 (61.9)	
Median (IQR)	1 (1 - 2)	3 (2 - 3)	
Infant Characteristics			
Sex			1.0
Female	6 (66.7)	12 (57.1)	
Male	3 (33.3)	6 (28.6)	
Missing	0 (0)	3 (14.3)	
Median gestation at delivery (completed weeks)	40 (40)	39 (38 - 39)	0.003
Birthweight in grams, Median (IQR)	3420 (3420 - 4000)	3305 (3010 - 3570)	0.07

642

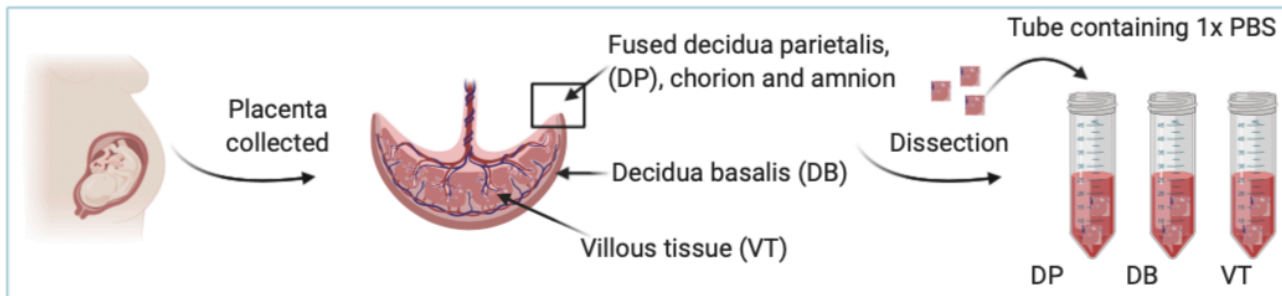
643

644 **Table 2: Placental characteristics and pathology at delivery**

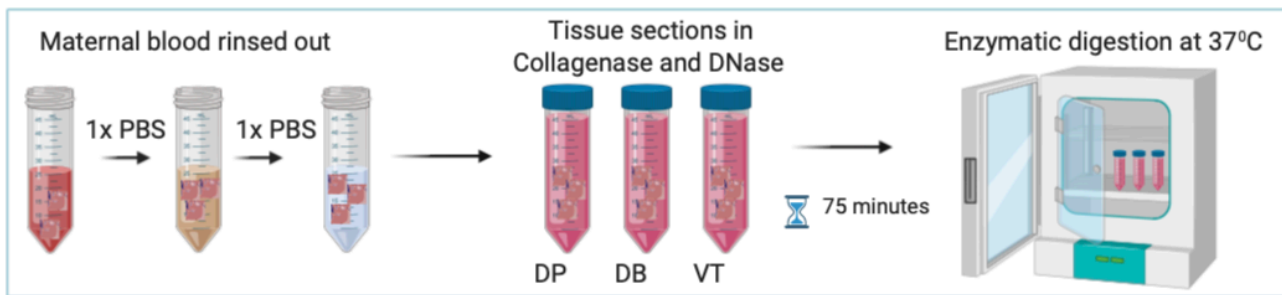
	PWNLHIV N=9	PWLWH N=21	P-Value
Placental basal plate weight (g), median (IQR)	468 (426 - 533)	394 (343 - 469)	0.02
Placental weight (g)			0.03
Small (<10 th percentile)	0 (0)	8 (38.1)	
Appropriate (10 - 90 th percentile)	9 (100.0)	12 (57.1)	
Large (>90 th percentile)	0 (0)	0 (0)	
Missing	0 (0)	1 (4.8)	
Fetal-Placenta weight ratio			0.02
Small (<10 th percentile)	1 (11.1)	0 (0)	
Appropriate (10 - 90 th percentile)	8 (88.9)	11 (52.4)	
Large (>90 th percentile)	0 (0)	7 (33.3)	
Missing	0 (0)	3 (14.9)	
Placenta greatest diameter (mm), median (IQR)	180 (172 - 210)	180 (170 - 199)	0.6
Placenta thickness (mm), median (IQR)	20 (15 -20)	25 (16.5 - 27.5)	0.2
Cord insertion			0.7
Central	3 (33.3)	3 (33.3)	
Off centre	5 (55.6)	12 (57.1)	
Marginal	1 (11.1)	5 (23.8)	
Missing	0 (0)	1 (4.76)	
Meconium exposure			0.1
+	3 (33.3)	2 (9.5)	
-	6 (66.7)	19 (90.5)	
Chorioamnionitis			
<i>Maternal Inflammatory Response</i>			0.6
+	2 (22.2)	2 (9.5)	
-	7 (77.8)	19 (90.5)	
<i>Fetal Inflammatory Response</i>			0.6
+	2 (22.2)	3 (14.3)	
-	7 (77.8)	18 (85.7)	
Chronic Deciduitis			0.5
+	0 (0)	2 (9.5)	
-	9 (100)	19 (90.5)	
Maternal Vascular Malperfusion			0.09
+	0 (0)	6 (28.6)	
-	9 (100)	15 (71.4)	
Villitis of Unknown Etiology			1.0
+	0 (0)	0 (0)	
-	9 (100)	21 (100)	

Figure 1

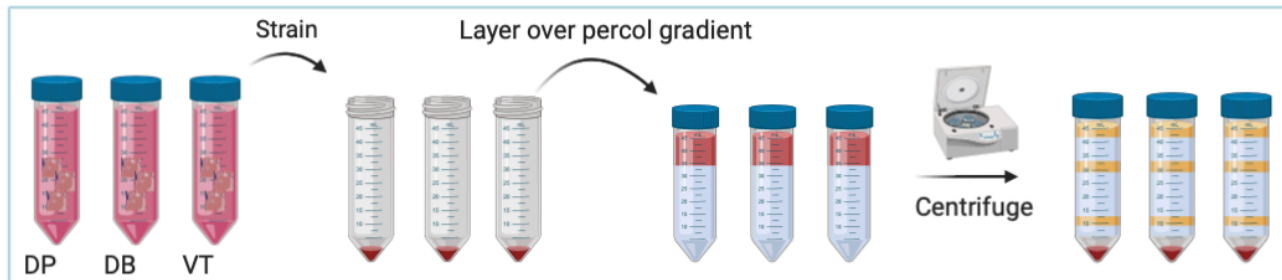
1 Dissection of the placenta



2 Rinsing out maternal blood and enzymatic digestion



3 Lymphocyte separation and collection



4 Cryopreservation and immunophenotyping

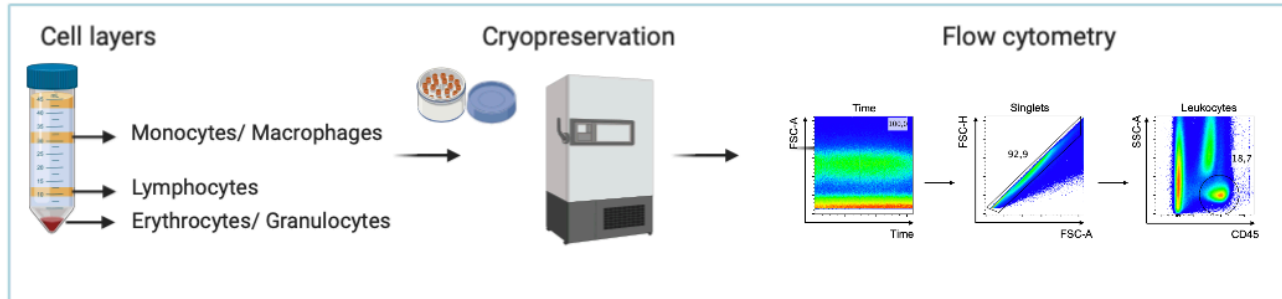
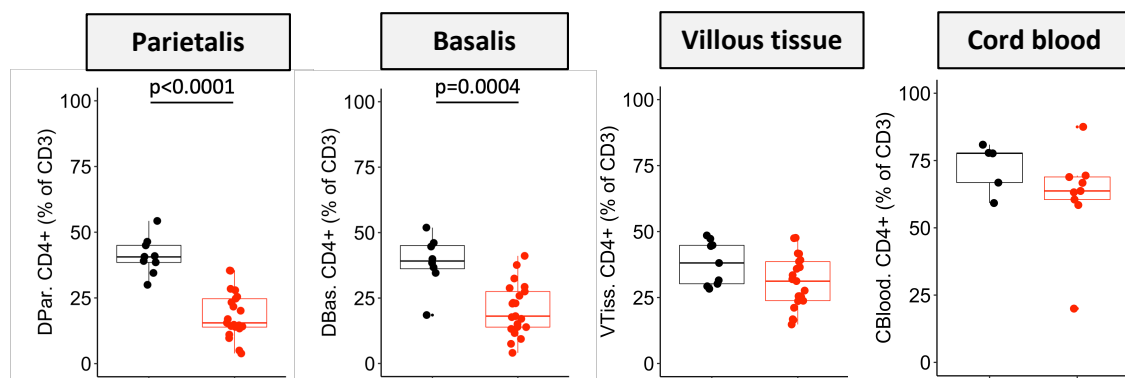
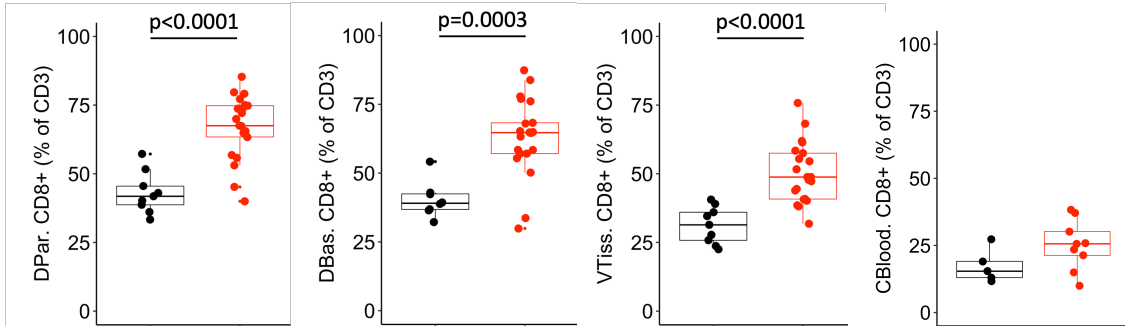


Figure 2

A CD3+CD4+CD8- T cells



CD3+CD4-CD8+ T cells



B CD4:CD8 T cell ratio

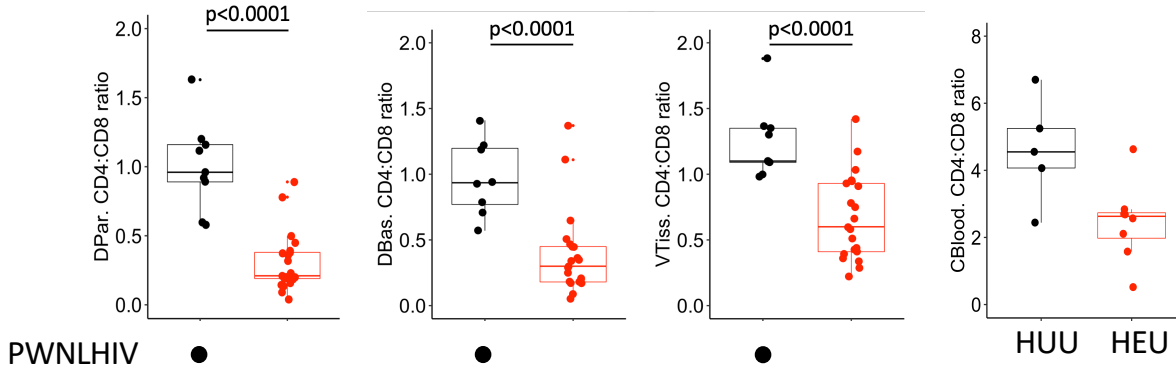


Figure 2

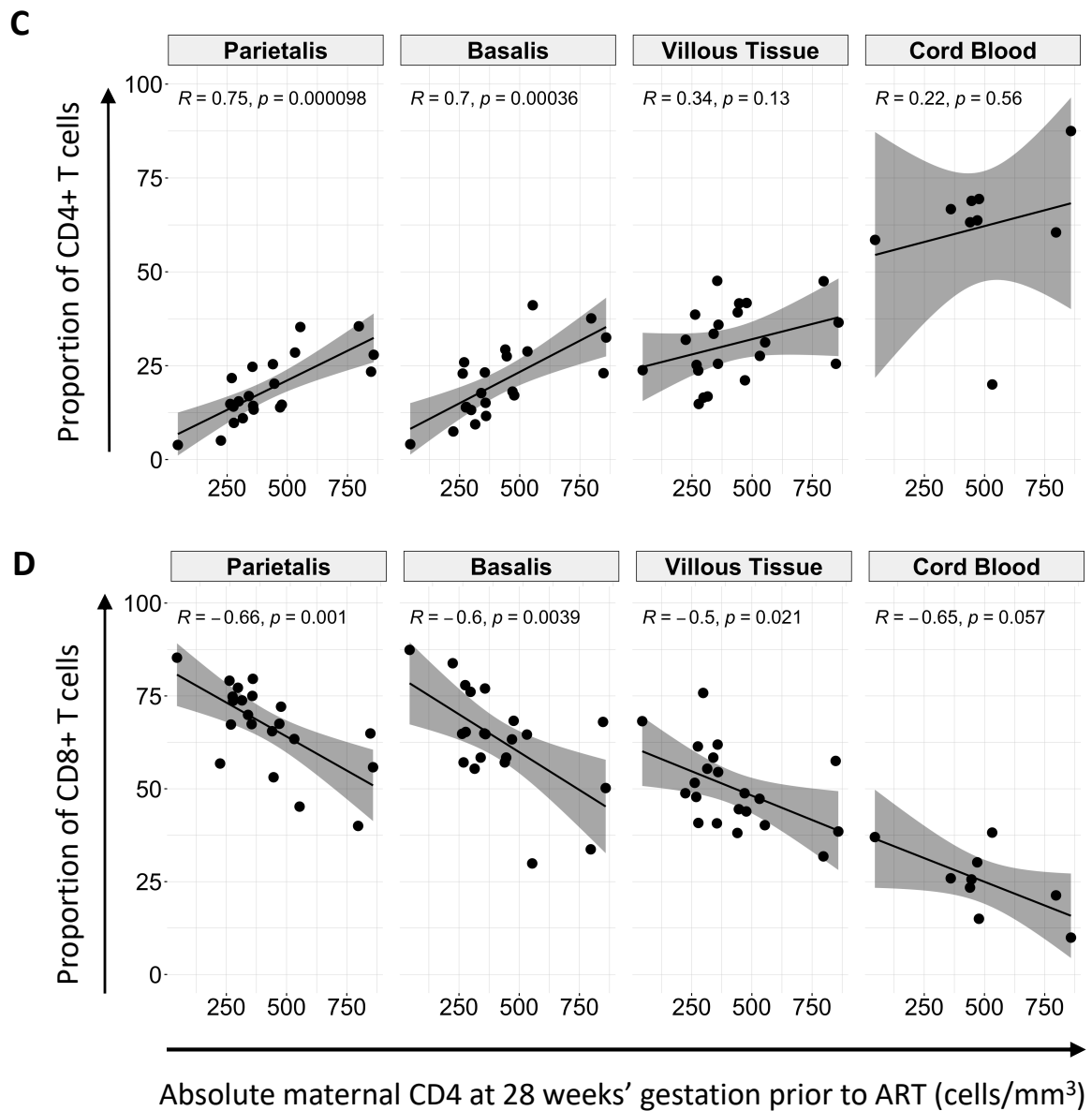


Figure 3

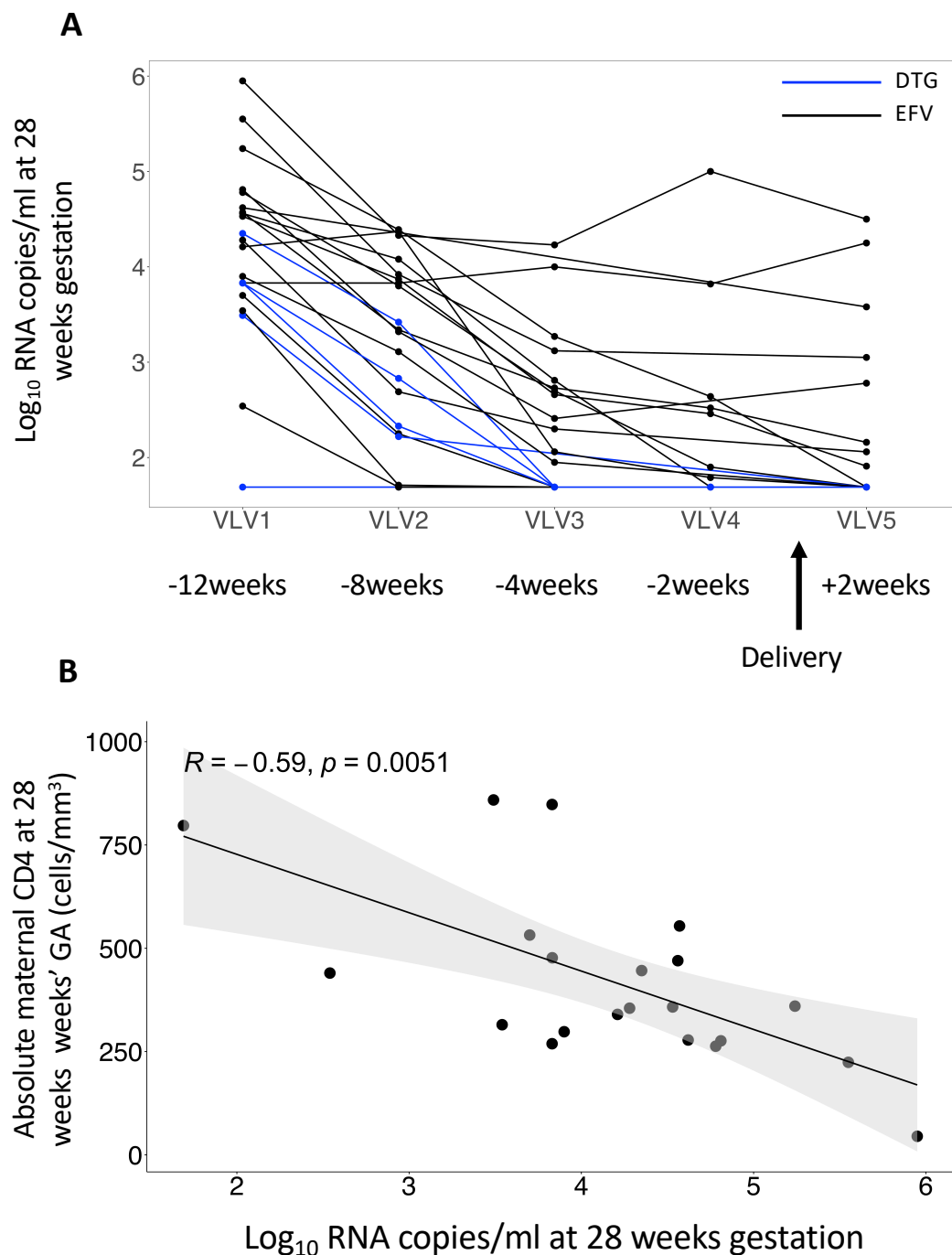


Figure 3

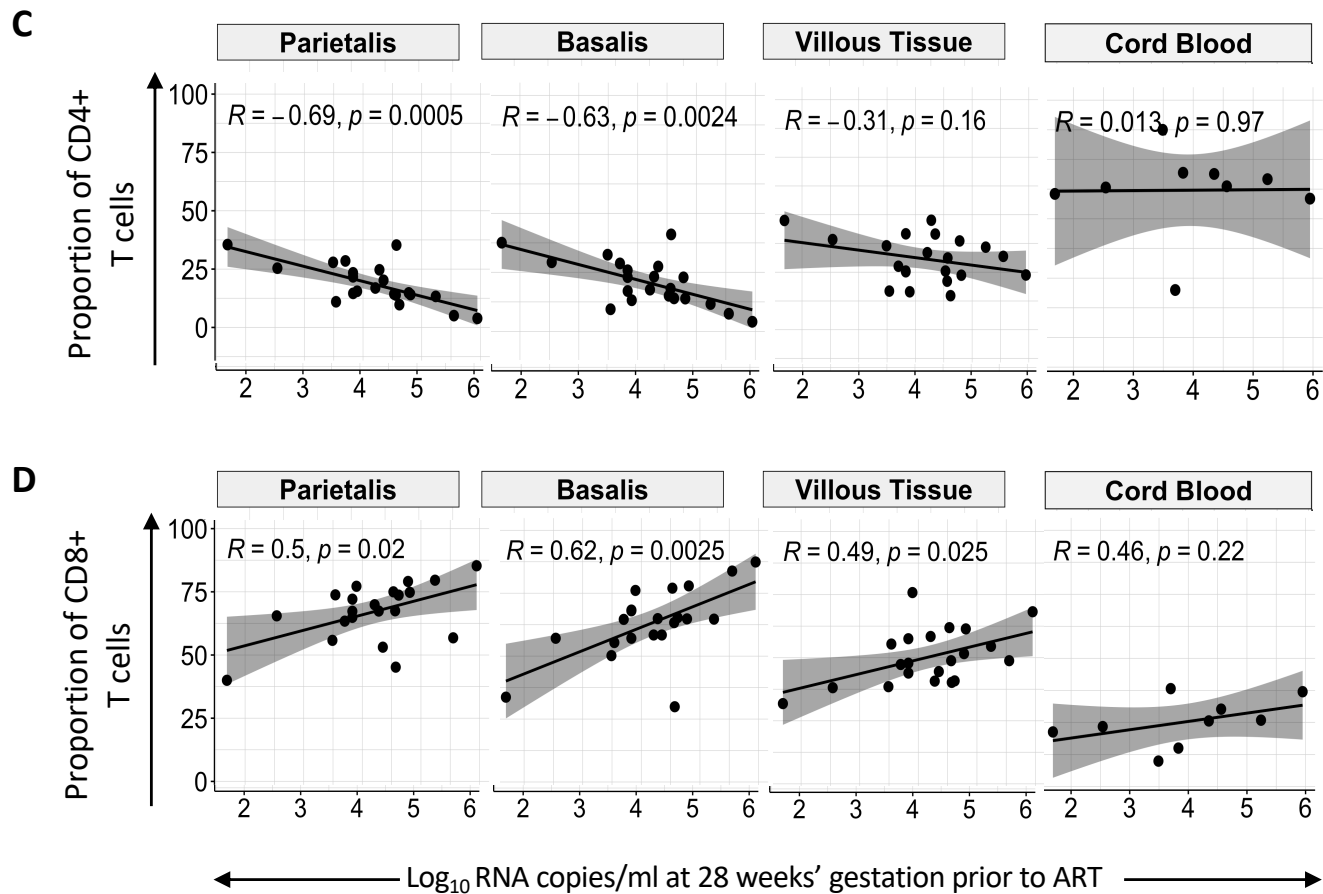


Figure 4

medRxiv preprint doi: <https://doi.org/10.1101/2021.01.04.21240108>; this version posted January 4, 2021. The copyright holder for this preprint (which was not certified by peer review) is the author/funder, who has granted medRxiv a license to display the preprint in perpetuity. It is made available under a CC-BY-ND 4.0 International license.

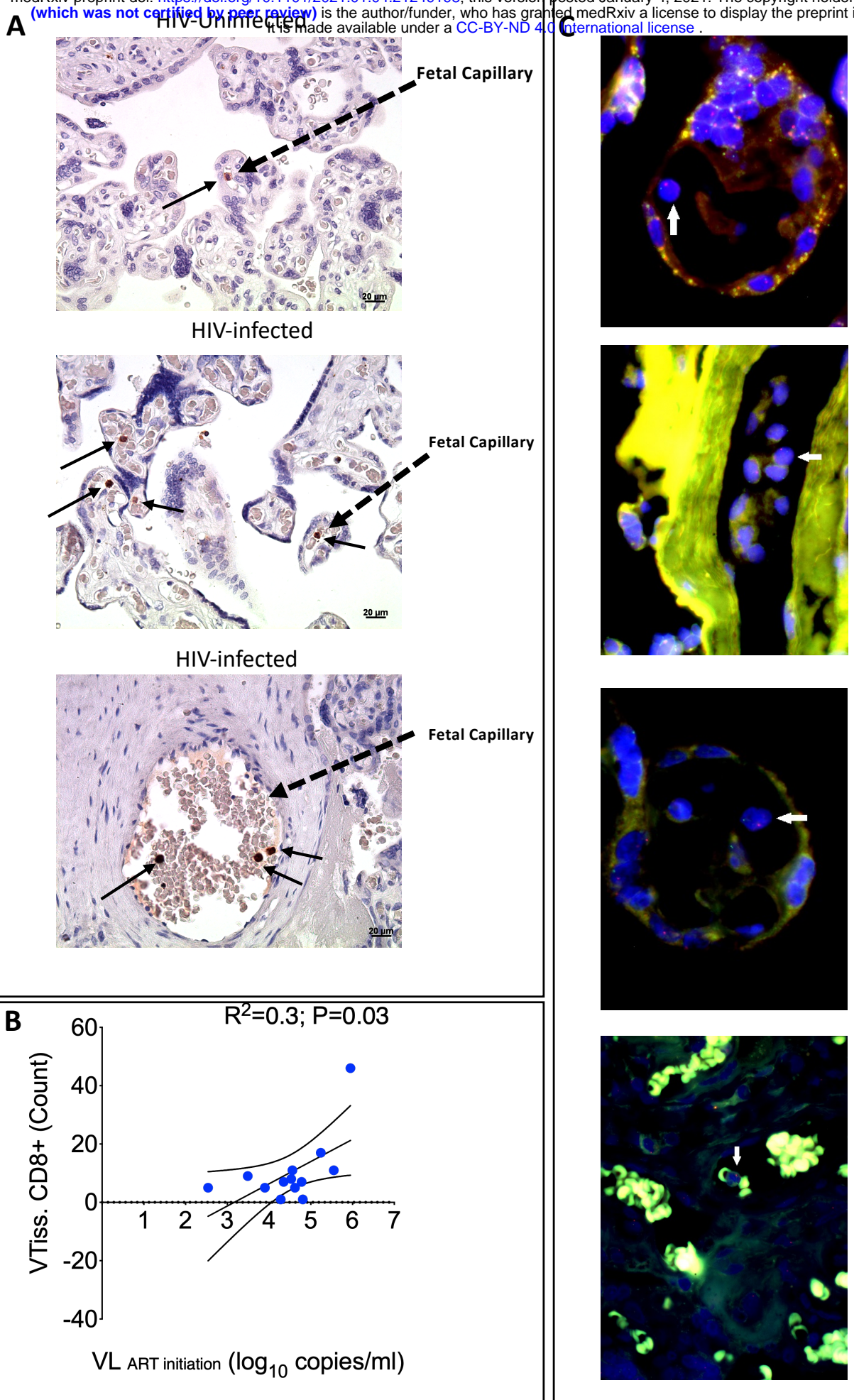
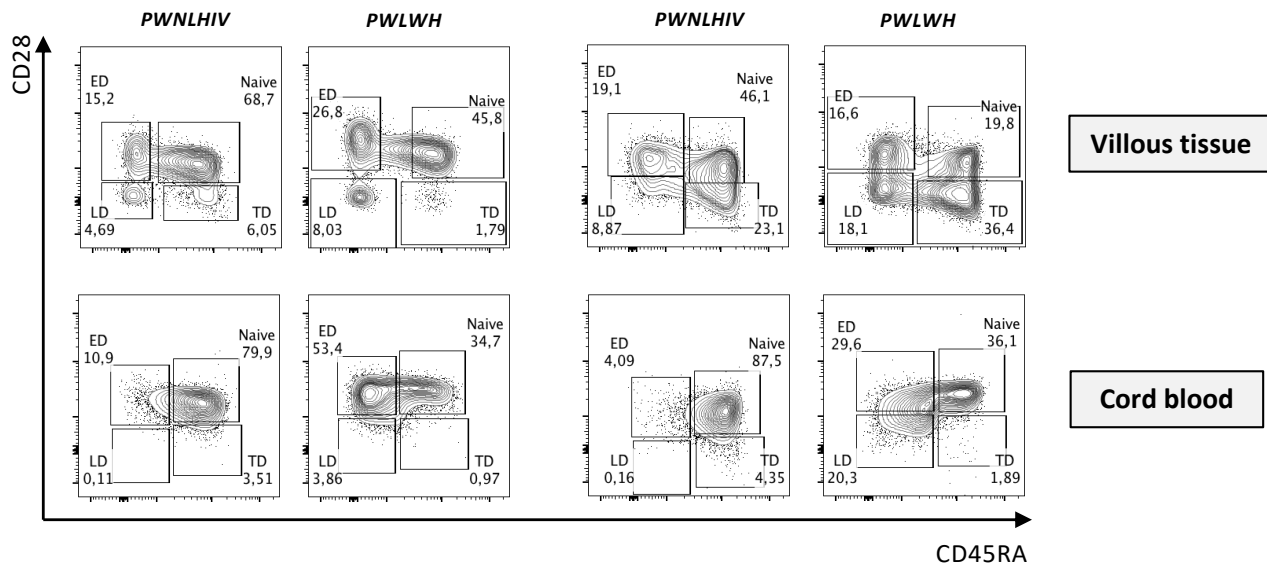


Figure 5

A CD3+CD4+ T cells



B

